



# Multiple therapeutic effects of human neural stem cells derived from induced pluripotent stem cells in a rat model of post-traumatic syringomyelia

Tingting Xu,<sup>a,\*</sup> Xiaofei Li,<sup>a</sup> Yuxi Guo,<sup>a</sup> Elias Uhlin,<sup>b</sup> Lena Holmberg,<sup>a</sup> Sumonto Mitra,<sup>c</sup> Dania Winn,<sup>b</sup> Anna Falk,<sup>b</sup> and Erik Sundström<sup>a,\*</sup>

<sup>a</sup>Division of Neurogeriatrics, Department of Neurobiology, Care Sciences and Society, BioClinicum J9:20, Karolinska Institutet, Stockholm, S17164, Sweden

<sup>b</sup>Department of Neuroscience, Karolinska Institutet, Stockholm, Sweden

<sup>c</sup>Division of Clinical Geriatrics, Department of Neurobiology, Care Sciences and Society, Karolinska Institutet, Stockholm, Sweden

## Summary

**Background** Post-traumatic syringomyelia (PTS) affects patients with chronic spinal cord injury (SCI) and is characterized by progressive deterioration of neurological symptoms. To improve surgical treatment, we studied the therapeutic effects of neuroepithelial-like stem cells (NESCs) derived from induced pluripotent stem cells (iPSCs) in a rat model of PTS. To facilitate clinical translation, we studied NESCs derived from Good Manufacturing Practice (GMP)-compliant iPSCs.

**Methods** Human GMP-compliant iPSCs were used to derive NESCs. Cryo-preserved NESCs were used off-the-shelf for intraspinal implantation to PTS rats 1 or 10 weeks post-injury, and rats were sacrificed 10 weeks later. *In vivo* cyst volumes were measured with micro-MRI. Phenotypes of differentiated NESCs and host responses were analyzed by immunohistochemistry.

**Findings** Off-the-shelf NESCs transplanted to PTS rats 10 weeks post-injury reduced cyst volume. The grafted NESCs differentiated mainly into glial cells. Importantly, NESCs also stimulated tissue repair. They reduced the density of glial scars and neurite-inhibiting chondroitin sulfate proteoglycan 4 (CSPG4), stimulated host oligodendrocyte precursor cells to migrate and proliferate, reduced active microglia/macrophages, and promoted axonal regrowth after subacute as well as chronic transplantation.

**Interpretation** Significant neural repair promoted by NESCs demonstrated that human NESCs could be used as a complement to standard surgery in PTS. We envisage that future PTS patients transplanted with NESCs will benefit both from eliminating the symptoms of PTS, as well as a long-term improvement of the neurological symptoms of SCI.

**Funding** This work was supported by Vinnova (2016-04134), Karolinska Institutet StratRegen, and the Chinese Scholarship Council.

**Copyright** © 2022 The Authors. Published by Elsevier B.V. This is an open access article under the CC BY-NC-ND license (<http://creativecommons.org/licenses/by-nc-nd/4.0/>)

**Keywords:** Neural stem cells; Transplantation; Spinal cord injury; Syringomyelia; Repair

## Introduction

Post-traumatic syringomyelia (PTS) is a chronic complication of spinal cord injury (SCI), characterized by progressive intraspinal cyst formation and expansion months to years after primary injury.<sup>1</sup> With the increased use of magnetic resonance imaging (MRI) for

diagnosis in the clinic the last two decades, the rate of diagnosed PTS in SCI patients has risen to 20–30%<sup>2</sup> but is still often an underestimated clinical problem.<sup>3</sup> The major symptoms are the aggravation of the already present functional impairment of movement, sensation and bowel or bladder control, and of other symptoms including neuropathic pain and spasticity.<sup>4</sup> The success rates of current surgical treatments, untethering with/without shunting, differ considerably between hospitals,

\*Corresponding authors.

E-mail address: [18243065861@163.com](mailto:18243065861@163.com) (T. Xu).

### Research in context

#### *Evidence before this study*

Post-traumatic syringomyelia is characterized by deterioration of neurological symptoms in the chronic stage of spinal cord injury. Current surgical treatment is not satisfactory, and the results differ significantly among clinics. A complementary therapy increasing the effectiveness of surgical treatment would be very important for post-traumatic syringomyelia patients. Considering the potential of stem cell therapy in central nervous system injuries, we recently performed and published the first experimental study showing that two types of human neural stem/progenitor cells both effectively reverse cyst expansion in a rodent model of post-traumatic syringomyelia. While our study showed a major effect on cyst volume, it is not known how cells transplanted to an intraspinal cyst will affect the surrounding parenchyma, and if they have effects on the injured host spinal cord that promote tissue repair. One of the cell types we studied previously was research-grade neuroepithelial-like stem cells derived from induced pluripotent stem cells manufactured from standard skin biopsies. For cell therapy in chronic conditions such as post-traumatic syringomyelia, clinically relevant neuroepithelial-like stem cells derived from the patient would be the preferred choice of cells. A key question is if the effect of transplanted neuroepithelial-like stem cells is limited to the cyst expansion, or if they have other therapeutic effects that could increase the repair of the injured spinal cord even in the chronic stage.

#### *Added value of this study*

To approach the clinical translation of cell therapy for post-traumatic syringomyelia patients, we applied neuroepithelial-like stem cells derived from Good Manufacturing Practice compliant- induced pluripotent stem cells, cryo-preserved and used as an off-the-shelf product for transplantation to a rodent post-traumatic syringomyelia model. The neuroepithelial-like stem cells transplanted to the chronic intraspinal cysts survived, proliferated initially with no signs of tumor growth, and reversed cyst expansion in rodent post-traumatic syringomyelia. We then investigated repair mechanisms of the neuroepithelial-like stem cells and found that they suppressed the glial scar surrounding the cysts, abolished the expression of chondroitin sulfate proteoglycan 4, reduced the number of active microglia/macrophages, stimulated proliferation of oligodendrocyte progenitor cells, and enhanced regrowth of descending serotonergic axons, all of which represent key elements in spinal cord tissue repair.

#### *Implications of all the available evidence*

The results strongly suggest that transplantation of neuroepithelial-like stem cells to the chronic spinal cord injury—post-traumatic syringomyelia patient will increase the effectiveness of the present standard surgical treatments and also stimulate the repair

mechanisms. Our data provide support for the first clinical trial of cell therapy for post-traumatic syringomyelia, to clarify if these patients will benefit from dual effects; reversing the cyst expansion to stop neurological deterioration and boosting the repair of the underlying spinal cord injury.

and some cysts recur after surgery.<sup>5,6</sup> Therefore, the development of additional treatments is important for PTS patients.

Neural stem/progenitor cell (NPC) transplantation studies have shown promising results for many neurological diseases both in animal models and clinical trials, particularly SCI.<sup>7–9</sup> NPCs from various sources can improve functional recovery in animal models of SCI, including NPCs derived from embryonic stem cells, adult or fetal spinal cords, and induced pluripotent stem cells (iPSCs), all with different advantages.<sup>10–12</sup> However, although NPCs from human fetal and adult spinal cords have shown promising effects in experimental SCI, there are concerns regarding sufficient access to tissue, immunosuppression after transplantation, and ethical concerns in some countries.<sup>13</sup> Neuroepithelial-like stem cells (NESCs) derived from iPSCs can provide an alternative as autologous transplantation reduces the risk for immune rejection and avoids most ethical concerns.<sup>14</sup> In a recent study, we applied this treatment and indeed showed that transplantation of NPCs or NESCs to intraspinal cysts in a rat PTS model effectively reverses the cyst expansion.<sup>15</sup>

Although reducing or eliminating the intraspinal cysts is the main clinical goal for a PTS treatment, the patients may benefit significantly from other effects of the transplanted cells having long-term effects on the underlying SCI. Experimental studies of SCI have shown that NPCs not only efficiently promote regeneration of severed axons, including cortical spinal cord tract and serotonergic axons but also can establish synaptic connections with host neurons leading to functional recovery.<sup>16–18</sup> However, these studies mainly focused on the acute-subacute phase of SCI while PTS patients are in the chronic phase. A few chronic phase transplantation studies showed treatment effects could only be achieved when combined with either modulation of inhibitory factors from host tissue or pretreatment of NPC with chemicals.<sup>18,19</sup> Here we show in a rat PTS model that NESCs derived from clinically relevant Good Manufacturing Practice (GMP)-compliant iPSCs not only prevent cyst formation when transplanted in the early stage and prevent cyst expansion when delivered into intraspinal cyst in the chronic stage, but also modulate the host tissue to a regenerative state by reducing the number of active microglia/macrophages and the astrogliosis surrounding the cyst, stimulate the presence of host oligodendrocyte progenitor cells (OPCs),

and enhance regeneration of descending serotonergic axons. Thus, cell therapy with NESCs shows broad potential as a treatment for PTS patients.

## Methods

### NESCs induction from dermal derived iPSCs

Dermal biopsies of volunteers were collected and dissociated mechanically and then enzymatically using 0.1% recombinant dispase II solution (Life Technologies #17105-041) prior to incubation at +4 °C for 16 h then followed by incubation with second enzyme 0.1% recombinant collagenase I solution, (Thermo Fisher Scientific #17100017) at +37 °C for 16 h. The digest was plated on 12 well tissue culture plates coated with CTG521 (Biolamina #CTG521) in Essential 8 medium (Essential 8, Thermo Fisher Scientific #A15169, +Penicillin-Streptomycin, Thermo Fisher Scientific #15140-122, + 20 ng/mL bFGF, Thermo Fisher Scientific #13256029). The digest (dermal Fibroblasts) was seeded on CTG521 coated 24 tissue culture plates and reprogrammed by mRNAs *OCT4*, *SOX2*, *KLF4*, *c-MYC*, *NANOG*, *LIN28*, StemRNA™-NM Reprogramming Kit (Stemgent/Reprocell #00-0076). Colonies were clonally expanded in Essential 8 Medium on CTG521 coated tissue culture plates. After reprogramming, iPS cells were plated on LN521 (Biolamina #LN521) coated tissue culture plates in Essential 8 medium and incubated for 24 h. Medium was changed to Knockout serum replacement (KOSR) medium (79% DMEM/F12 + GlutaMax Gibco, #31331-028, 20% KnockOut Serum, Gibco, #10828028, Non-essential Amino Acids, Gibco, #11140-076, 2-mercapthoethanol, Gibco, #31350-010, Penicillin-streptomycin, Gibco, #15140-122, 10 nM of SB-431542 StemCell Technologies #72232, 500 ng/mL of Noggin, PreproTech #120-10C and CHIR, StemCell Technologies #72052). KOSR medium was changed every 24 h. Cells were passaged 5 days after plating and 125,000 cells were seeded in a new well of LN521 coated tissue culture plate. From passage, SB431542 was removed from the medium and the KOSR medium was mixed with an increasing level of N2B27 medium (DMEM/F12 GlutaMax, Neurobasal, Gibco, #21103-049, 2-mercapthoethanol, N2, Gibco, #17504-044, B27, Gibco, #17502-048 and Penicillin-streptomycin) to be fully replaced by N2B27 medium by day 10. On day 12, the cells were passaged and cultured as NES cells.

### NESCs culture and differentiation *in vitro*

NESCs were cultured on PLO and laminin2020-coated flask in the growth medium (DMEM/F12 Glutamax supplemented with 1% N2, 0.1% B27, FGF 10 ng/μl, EGF 10 ng/μl, Peprotech #AF-100-15, and 1% Penicillin-Streptomycin Thermo, #15140-122). When confluent, the cells were detached from the bottom of the flask using TrypLE select (Invitrogen # 12563) and split 1:3.

NESCs were differentiated as an adherent culture in differentiation medium (DMEM/F12 Glutamax supplemented with 1% N2 and 1% B27) without any supplement of growth factors.

## Trypan blue was used to evaluate the viability of NESCs

### Animals and injury model

Female Sprague-Dawley rats (Charles River, 180-220 g) were used for injury model and cell transplantation treatment. All animal procedures were in accordance with the Swedish Animal Protection Act and approved by the Regional Ethics Committee on Animal Research, Stockholm, Sweden.

Rats were given Atropin (0.05 mg/kg, NM Pharma AB) i.p. 10–15 min before anesthesia and then put under anesthesia for the whole surgical procedure by isoflurane inhalation (3% for induction and 1.75% for maintenance, oxygen rate 500 ml/min). Core body temperature was kept at 37 °C with a rectal probe and heating pad. 6 ml Ringer's solution with 5% glucose was given subcutaneously both before and after injury. PTS was induced as previously described(15). Briefly, laminectomy was performed at spine level Th9, and mild contusion injury inflicted by the Infinite Horizon impactor (Precision Systems and Instrumentation, LLC) (force = 100 kdyn) on the exposed dorsal spinal cord at spinal cord level Th10-11, followed by subarachnoid injection of 100 μl venous blood from the tongue vein. Artificial dura (Lyoplant, B/Braun Aesculap AG) was then placed to cover the opening of dura before the wound was closed with sutures layer by layer. Temgesic (buprenorphine, 7 μg/kg s.c., Reckitt& Colman) were given subcutaneously twice a day for 4 days, and the bladder was emptied manually until spontaneous evacuation was stable.

For subacute transplantation, rats were randomly divided into NESC ( $n = 11$ ) and vehicle groups ( $n = 6$ ). For chronic transplantation, rats with cyst volumes larger than 2 mm<sup>3</sup> based on the pre-transplantation MRI were selected, since cysts smaller than 2 mm<sup>3</sup> usually heal spontaneously. Rats were assigned to NESC ( $n = 7$ ) and vehicle ( $n = 7$ ) groups based on the pre-transplantation MRI in order to achieve similar cyst volumes in the two groups.

## Experimenters were blinded when performing data analysis

### NESCs preparation and transplantation

NESCs were thawed in water bath and then washed and resuspended twice with DMEM/F12 medium and their viability was tested with trypan blue. Then NESCs were resuspended with injection medium, DMEM/F12, to

100,000 viable cells/ $\mu\text{l}$ . Cyclosporin (Sandimmun, 10 mg/kg s.c., Novartis) was administered daily to all rats (NESCs and vehicle groups) starting from 1 day before the transplantation until the endpoint. Either 1-week or 10-week post-injury, the laminectomy area was cut open and 3  $\mu\text{l}$  NESCs suspension in DMEM/F12 medium (100,000 cells/ $\mu\text{l}$ ) or 3  $\mu\text{l}$  DMEM/F12 only was slowly injected into the parenchyma at the lesion site (1 week) or into the cyst (10 weeks) guided by pre-operative MRI. The preparation before and care of rats after surgery were the same as previously described.<sup>15</sup>

#### Immunohistochemistry staining and imaging

Rats were anesthetized with Pentobarbital (60 mg/kg) before decapitation and then the spinal cord were dissected, collected, and then immersed in 4% PFA for 24–36 h followed by immersion in 10% and 30% sucrose, each for 24 h. The injury site of spinal cords was embedded in O.C.T compound (Tissue-Tek), rapidly frozen and sectioned longitudinally or coronally with a section thickness of 10  $\mu\text{m}$ .

#### Cultured cells were fixed with 4% PFA for 10 min, followed by 5 quick rinses with MilliQ water before primary antibody incubation

For immunofluorescent staining, sections or cells were washed in PBS for 10 min and then incubated in primary antibody diluted in blocking buffer (PBS with 10% normal donkey serum and 0.3% triton X-100) at room temperature overnight. The primary antibody used were: NeuN (Sigma, HPA030790, 1:300), GFAP (DAKO, Z0334, 1:500), GFAP (Abcam, AB4648, 1:200), Sox9 (R&D systems, AF3705, 1:300), Olig2 (R&D systems, AF2418, 1:300), Sox2 (Millipore, AB5603, 1:1000), Ki67 (DAKO, M7240, 1:100), HuNu (Millipore, MAB1281, 1:100), HSP27 (Stressgen, SPA-803, 1:1000), CC1 (calbindin, OP80, 1:250), Glast (Chemicon, AB1782, 1:1000), S100A10 (Thermo, PA595505, 1:250), ED1 (Bio-Rad, MCA341R, 1:100), 5HT (Abcam, ab66047, 1:500), AQP 4 (Sigma, HPA014784, 1:500), IL1 $\beta$  (R&D systems, AF-501-NA, 1:20), TNF $\alpha$  (R&D systems, AF-510-NA, 1:20), IL1RA (gift from Dr. Stefan Svensson lab, rabbit, 1:100). After incubation, sections were washed once in PBS and then incubated with the corresponding donkey-derived secondary antibodies (Alexa488, Cy3, or Alexa647 conjugated) for 1 hour. After secondary incubation, sections were washed with PBS-T (PBS, with 0.05% tween 20) for 10 min, counterstained with DAPI (1:2500) for 1 min before a final rinse in PBS-T before mounting with PVA-DABCO.

Tissue sections were imaged with a Zeiss LSM 700 confocal microscope with Plan Apochromat 20X/C-Apochromat 40X objectives using Zen software (Zen Black 2010 v6.0.0.309). Cell cultures were imaged with

a widefield microscope (Zeiss Celloobserver) and images were acquired by Zeiss AxioCam camera and created using Zen software (Zeiss Zen 2 (Blue) v2.3). All the images were processed and quantified using ImageJ.

#### Flow cytometry

NESCs were detached from the culture plates with TrypLE select and resuspended with stain buffer (BD Pharmingen, #554656) (containing 0.5% BSA) and for cell counting to have 200 000–400 000 cells per sample. Fixed with fixing reagent, 100  $\mu\text{l}$  (ThermoFisher, #00-5123 part of kit #00-5523-00) for 15 min at room temperature after centrifuge and discarded the supernatant. Cells were permeabilized with permeabilization buffer (ThermoFisher, #00-8333 part of kit #00-5523-00) 150  $\mu\text{l}$  per tube and removed supernatant after centrifuge. Incubated in permeabilization buffer with Sox2-Alexa488 (BD, #560301) antibody for 20 min at room temperature. Washed once with stain buffer and resuspended with stain buffer before loading into Accuri Plus flow cytometer (BD). Cells were identified as follows: Sox2 positive were considered as neural stem cells, Sox2 negative were considered as progenies of neural stem cells. All events were gated based on viable and single cells.

#### Micro-MRI scanning of the rat spinal cord *in vivo*

MRI was performed using a horizontal 9.4 T magnet (Varian, Yarnton, UK) with a 31 cm bore. A 72 mm volume coil was used for transmission, in conjunction with a four-channel phased array surface receive coil (RapidBiomed, Würzburg, Germany).

Rats were anesthetized with isoflurane and body temperature was kept at 37 °C during anesthesia. The rats were placed in the micro-MRI machine with monitoring of heart and breathing rate. Acquisition of the MRI images as well as analysis of the images to measure length and volume of the intraspinal cyst was performed as previously described<sup>(15)</sup>. Briefly, by using ImageJ software (NIH), the T2 weighted transverse images with hyperintense signal in the spinal cord were converted to 8-bit format images and then the threshold was set based on the grayscale to include and highlight the pixels representing cystic fluid (white) in spinal cord and exclude the remaining pixels representing tissues. The area of each image was measured, summed, and multiplied by the thickness of transverse image (0.5 mm) to get the total volume of the cyst.

#### Quantitative analysis

For counting transplanted cells, a series of 10  $\mu\text{m}$  cryostat sections covering the entire region of transplanted cells, interval 1:40 was taken, and all HuNu positive cells were counted in each section. The total number of

transplanted cells ( $N$ ) were obtained using the following equation:

$$N = k/2 * \sum_{(i=1)}^n x_i$$

$k$  is the number of section intervals;  $x$  is the number of HuNu positive cells in each section. In our case,  $k$  equals 40.

For phenotype analysis of transplanted cells, cells positive for HuNu and either of the following markers, NeuN, Olig2, Sox9, and Sox2 were counted.

Quantification of the area of host GFAP immunoreactivity and number of ED1 positive microglia/macrophages were done in one section from the epicenter.

Regarding the serotonin (5-HT) staining analysis, sections 2 mm caudal to the lesion site and 1mm rostral to the lesion site were chosen, and the ratio of serotonin density along the midline between them was referred to as serotonin index.

## Ethics

Skin biopsies from healthy volunteers, acquired with permission from the Regional Ethical Committee (Ethical number: 2012/208-31/3), Stockholm, were used to produce iPSCs. No material acquired from prisoners was used.

All procedures regarding experimental animals were approved by the Regional Committee on Research Animals Ethics Committee, Stockholm (Ethical number: 1733).

## Statistical analysis

The statistical comparison included two-tailed  $t$ -test, one-way ANOVA, and Fisher's exact test as specified in the figure legends using Prism software. All the data analyses above were used as indicated. Statistical significance was indicated as \*  $p < 0.05$  and \*\* $p < 0.01$ . Shapiro-Wilk test (GraphPad Prism) was applied for the normality test.

## Role of funders

This work was supported by Vinnova (2016-04134), Karolinska Institutet StratRegen, and China Scholarship Council (CSC). The funders had no role in the experimental design, collection of data or writing of the paper.

## Results

### *In vitro* evaluation of NESCs derived from GMP-compliant iPSCs

To avoid batch-to-batch effects and thereby gain more reliable results, we prepared a large amount of GMP-

compliant iPSC-derived NESCs for transplantation and cryopreserved them in standardized doses. We evaluated the viability of NESCs before transplantation and found high viability after recovery from cryopreservation, enabling them to be applied off-the-shelf after cryopreservation in the present study (Figure 1 a). Next, we analyzed the differentiation property of NESCs and found that the percentage of stem cells (Sox2 positive cells) decreased upon differentiation from day 0 (D0) to 12 (D12), in line with the expected differentiation of NESCs, progressive loss of stemness and differentiation to neural lineages with the expression of b-tubulin type III at D12 (Figure 1 b and c). These findings showed that NESCs have the potential to replace lost cells, including neurons, after transplantation to the parenchyma of injured spinal cord.

### Transplanted NESCs counteract cyst formation and expansion *in vivo*

In our previous study, we generated a rat model of PTS with progressively expanding cysts in chronic SCI and showed that these cysts could be efficiently reversed by transplantation of research-grade fetal spinal cord derived NPCs and NESCs.<sup>15</sup>

To closer mimic the clinical situation, we performed chronic transplantation with clinically relevant NESCs to further move forward to clinical translation. In addition, to investigate if promoting endogenous repair is a general effect by NESCs, we also transplanted NESCs in the subacute phase, 1 week after injury to PTS rats and analyzed the animals 10 weeks after transplantation by evaluating cyst formation using immunohistology analysis, delineating the cyst by the distribution of GFAP positive cells (Figure 2 a and b). We found that only 9.1% of rats had developed cysts in the NESCs group compared to 83.3% of rats in the vehicle group, showing that subacutely transplanted NESCs efficiently prevent the formation of cysts and with neural tissue preservation (not filling effect) in our rat PTS model (Figure 2 c).

For the chronic transplantation study, we used micro-MRI to monitor the size change of intraspinal cysts. The cysts had the same brightness as CSF with a clear border to the spared tissue (Figure 2 e and S1). To evaluate how NESC transplantation affects cyst size over time in PTS, the spinal cord of rats from the NESCs group and vehicle group were scanned with micro-MRI the week before transplantation and 10 weeks after transplantation (Figure 2 d). We observed significant differences between NESCs and vehicle groups. The cyst volumes decreased on average by 84.4% in the NESCs group, while the volume of cysts increased by 75.3% in the vehicle group (Figure 2 f). In addition, the length of cysts in NESCs group was



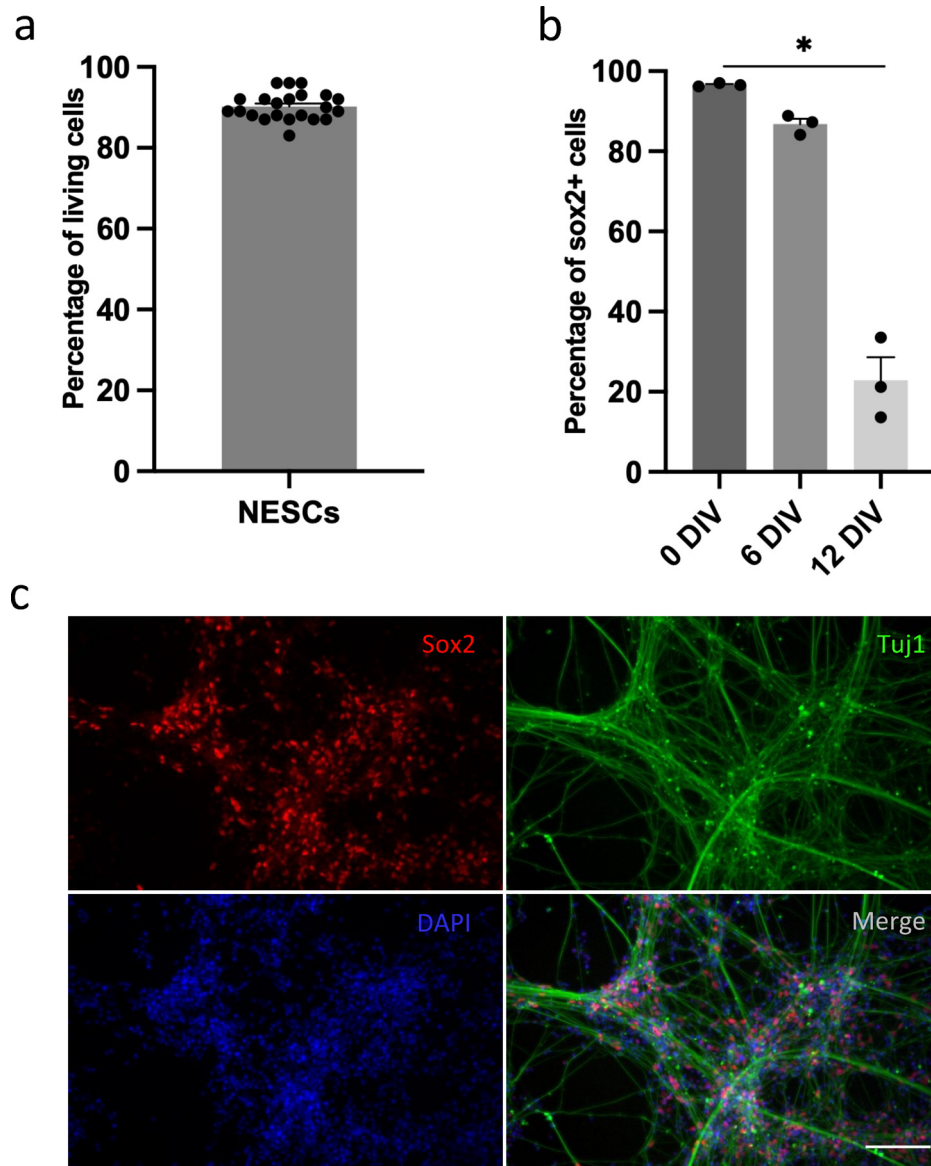


**Figure 1. Phenotypes of NESCs at different differentiation stages *in vitro*.** (a) Quantification of living cells of cryopreserved NESCs. (b) Quantification of Sox2 positive cells at three different stages of differentiation *in vitro*, 0 DIV, 6 DIV and 12DIV (mean ± SEM, one-way ANOVA,  $p < 0.05$   $n = 3$  batches of cells per group). (c) Differentiated NESCs (12 days *in vitro*) stained for Sox2 (red), beta III tubulin (Tuj1, green) and DAPI (blue). Scale bar = 30 μm.

reduced by 25.6%, while it increased by 2.0% in the vehicle group (Figure 2 f), thus confirming the therapeutic effect of NESCs.

### Survival and proliferation of NESCs in PTS rats *in vivo*

To investigate how the transplanted human NESCs survive and proliferate in the host tissue, we quantified the number of NESCs with human specific nuclear marker

(HuNu), and the ratio of NESCs expressing the proliferative marker Ki67, 10 weeks after subacute and chronic transplantation.

The long-term survival of transplanted cells was high after both subacute and chronic transplantation, exceeding the original number of transplanted cells (300,000), with significantly more cells after chronic transplantation (Figure 3 a). In agreement with this, we found that transplanted NESCs proliferated *in vivo*, about 30% of NESCs transplanted subacutely were proliferating, as indicated by Ki67 expression, 1 week after

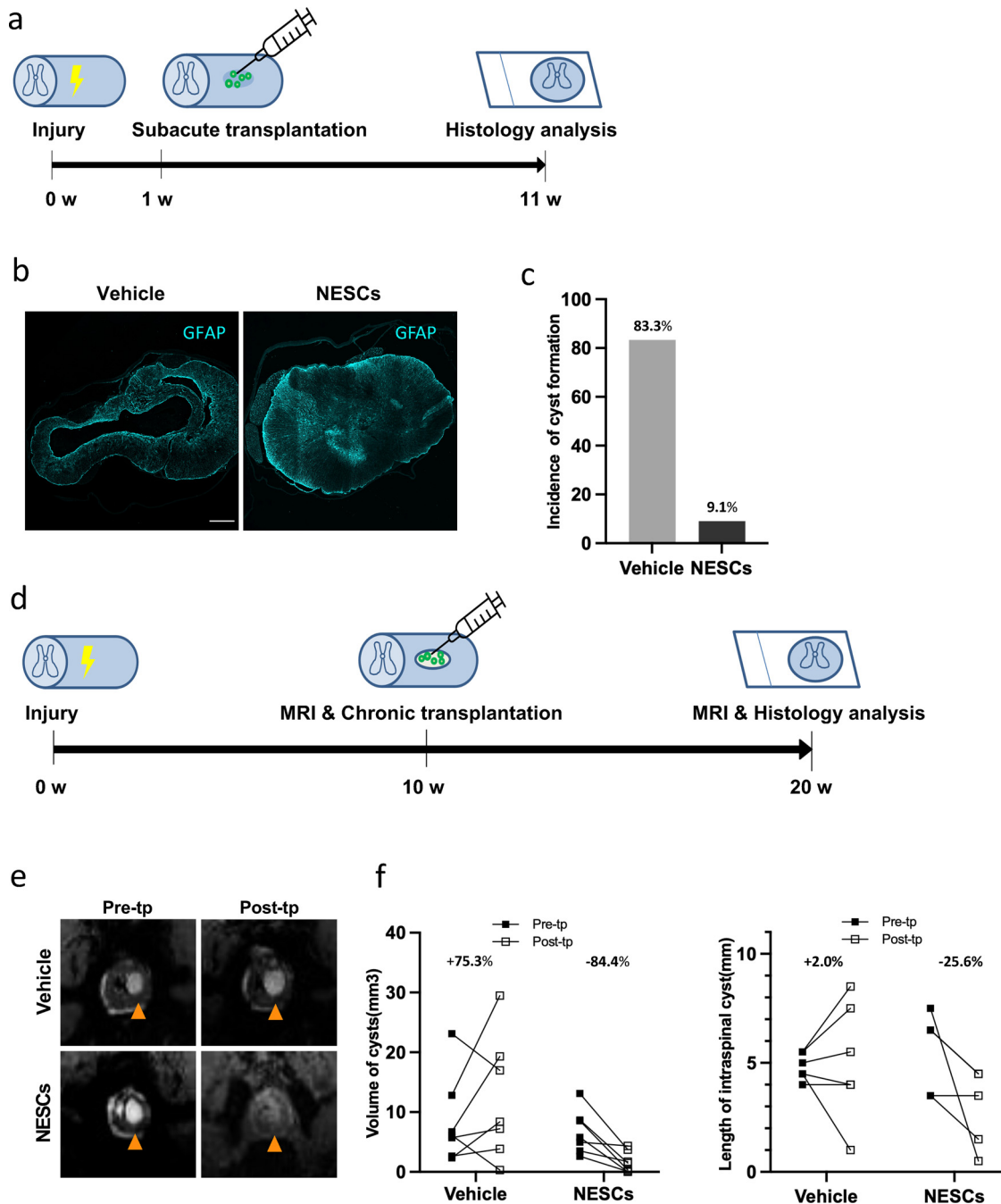


**Figure 2.** Clinically relevant iPSC-NESCs have potent treatment effects on PTS cysts after subacute as well as chronic transplantation. (a, d) Experimental design of subacute and chronic transplantation, respectively. (b) Spinal cord sections of the lesion site from vehicle and NESC groups stained for GFAP (cyan). Scale bar = 300  $\mu$ m. Section thickness = 10  $\mu$ m. (c) The incidence of cyst formation in vehicle and NESC groups after subacute (1 week) transplantation (Fisher's exact test,  $p < 0.01$ ). (e) MRI of pre- and post-transplantation from vehicle and NESC groups of chronic (10 weeks) transplantation. (f) The changes of cyst volume and length pre- and post-transplantation in vehicle and NESC groups of chronic transplantation. MRI, magnetic resonance imaging; Pre/post-tp, pre/post-transplantation. Sp.c, spinal cord.

transplantation (Figure 3 b). Notably, only 2–5% of the transplanted cells were Ki67 positive 10 weeks after transplantation (Figure 3 c), confirming no continuous

overgrowth concern of these transplanted cells. Most of the NESCs were located at the transplantation sites 10 weeks after both subacute and chronic transplantation.

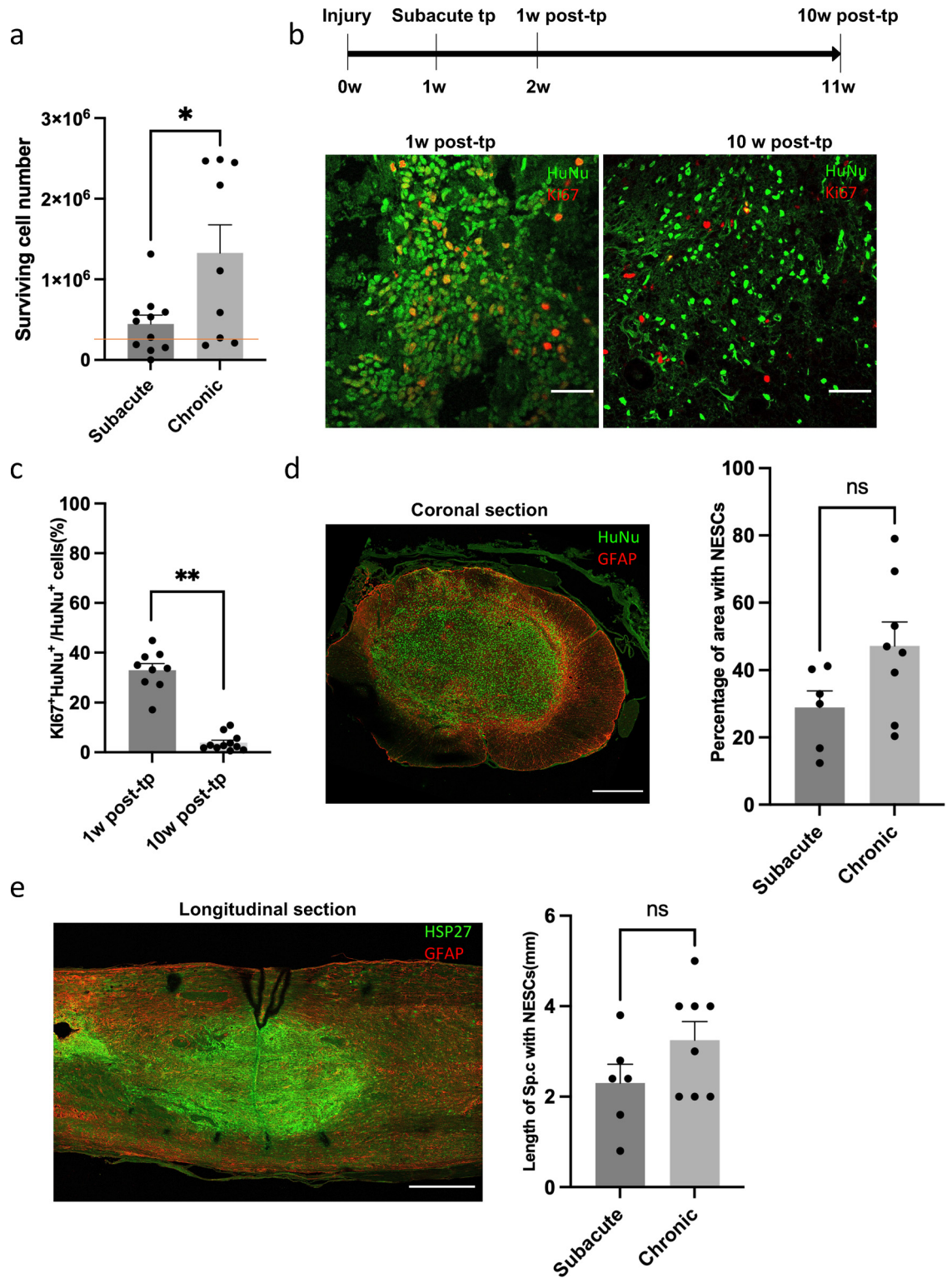


**Figure 3. Survival and proliferation of transplanted cells.** (a) Cell number count of NESCs 10 weeks after subacute transplantation and chronic transplantation (mean ± SEM, two-tailed t-test,  $p < 0.05$ ,  $n = 11$  and  $9$  rats, respectively). The red line indicates the number of transplanted NESCs. (b) Coronal spinal cord sections of the transplantation site from 1 week and 10 weeks post-transplantation, respectively stained for HuNu (green) and ki67 (red). (c) Quantification of Ki67 positive NESCs 1 week and 10 weeks after



The transplanted cells were mainly located at the inner 1/3–1/2 of area of the coronal spinal cord section, and over a length of 2–3 mm (NESCs labeled by human specific marker, HSP27), with no significant differences between subacute and chronic transplantation conditions (Figure 3 d and e). In order to verify the long-term stability of grafted cells, we quantified their survival at 15 weeks after transplantation. We observed no reduction of survival cell number between 10 and 15 weeks after transplantation, and no differences in their distribution in the host spinal cord (Figure S2 a–d).

### Characterization of transplanted NESCs *in vivo*

To verify that NESCs can differentiate into multiple neural cells after intraspinal transplantation, we next quantified the differentiation of NESCs and their progeny 10 weeks after transplanting NESCs to the injured parenchyma at the subacute stage, or to the identified cysts in chronic PTS. We used NeuN, Olig2, Sox9, and Sox2 to label neurons, oligodendrocyte lineage cells, astroglial lineage cells, and neural stem cells, respectively (Figure 4 a). We found that in rats with NESCs transplanted to chronic PTS cysts 40% of NESCs remained as neural stem cells, 40% developed into astroglial lineage cells, 10% into neurons and 2% into cells of the oligodendrocyte lineage cells, i.e., oligodendrocytes and OPCs (Figure 4 c). In rats transplanted subacutely, a smaller proportion remained as Sox2 positive (18%), but the proportion of cells positive for other markers was also lower than chronic transplantation (17%, 7%, and 2%, respectively). We further investigated vimentin expression in the undefined cells and found that the majority were Vimentin positive and some of them were Vimentin<sup>+</sup>/Sox2<sup>-</sup>, indicating that these cells may have left the stem cell state, but their fates have not been defined yet (Figure 4 c and S3). In an analysis conducted 15 weeks after transplantation (25 weeks post-injury) we found a similar differentiation situation (Figure S2 e and f). The maturation of glial NESC progeny was verified by immunostaining for the astrocyte glutamate transporter GLAST and oligodendrocyte marker CC1 in HuNu positive cells (Figure 4 f).

Although there were very few OPCs/oligodendrocytes derived from transplanted NESCs, we found an even and abundant distribution of Olig2 positive cells of which 73% were derived from the host tissue,

intermingled with the transplanted human cells (Figure 4 a, b and S4). The percentage of resident OPCs (Olig2<sup>+</sup>Ki67<sup>+</sup>HuNu<sup>-</sup>) that were proliferating in the NESCs group were two to four times higher than in the vehicle group, indicating that transplanted NESCs promote proliferation of endogenous OPCs (Figure 4 d and e).

### Modulation of astrocytes and active microglia/macrophages by transplanted NESCs

In response to spinal cord trauma, astrocytes become reactive with increasing expression of GFAP, followed by the formation of a well-defined astrocytic scar around the lesion site. Studies have shown that scar-forming astrocytes are different from reactive astrocytes in gene expression profiles.<sup>20</sup> In accordance, the PTS cysts were surrounded by scar-forming astrocytes expressing a high level of GFAP and low level of S100A10, with reactive astrocytes in adjacent intact tissue expressing a high level of S100A10 and a lower level of GFAP (Figure 5 a). We then investigated whether scar-forming astrocytes and reactive astrocytes were modulated by NESCs, respectively. We found an absence of astrocyte scar tissue around the cyst in the NESCs group in sharp contrast to the vehicle group in both subacute and chronic transplantation conditions (Figure 5 c). We also quantified the density of total GFAP positive astrocytes at the lesion site and found that the density was significantly lower in the NESCs group compared to the vehicle group after subacute transplantation. However, no difference was observed in chronic transplantation (Figure 5 c and d). Aquaporin 4 is the most abundant aquaporin in the spinal cord, mainly localized to astrocytic endfeet, and plays an important role in water homeostasis. It has been shown that aquaporin 4 plays a negative role in functional recovery following SCI and its expression increases adjacent to the cyst from the acute phase to the chronic phase in a rat model of PTS.<sup>21,22</sup> We found that NESCs transplantation resulted in a significantly lower density of astrocytic aquaporin 4 on cell membrane than vehicle after both subacute and chronic transplantation (Figure S5).

Closely associated with the glial response to injury are the chondroitin sulfate proteoglycan (CSPGs), molecules inhibiting axonal regrowth in the adult central nervous system with CSPG4 as an important

subacute transplantation. (mean ± SEM, two-tailed t-test,  $p < 0.01$ ,  $n = 8$  and 10 rats, respectively). (d) Coronal spinal cord sections of transplantation sites from rats with NESCs transplanted to chronic intraspinal cysts, double stained with human specific marker HuNu (green) and GFAP (red). Quantification of the distribution of NESCs 10 weeks after subacute transplantation and chronic transplantation in the ventral-dorsal plane (mean ± SEM, two-tailed t-test, no statistical significance,  $n = 6$  and 8 rats, respectively). (e) Longitudinal spinal cord sections of transplantation sites from chronic transplanted rats with NESCs transplanted to intraspinal cysts, double stained with human specific marker, HSP27 (green) and GFAP (red) Quantification of the distribution of NESCs 10 weeks after subacute transplantation and chronic transplantation in the rostral-caudal plane (mean ± SEM, two-tailed t-test, no statistical significance,  $n = 6$  and 8 rats, respectively). Scale bar = 50 μm in b; Scale bars = 300 μm for coronal section and 400 μm for longitudinal section in d. Section thickness = 10 μm. Post-tp, post transplantation.

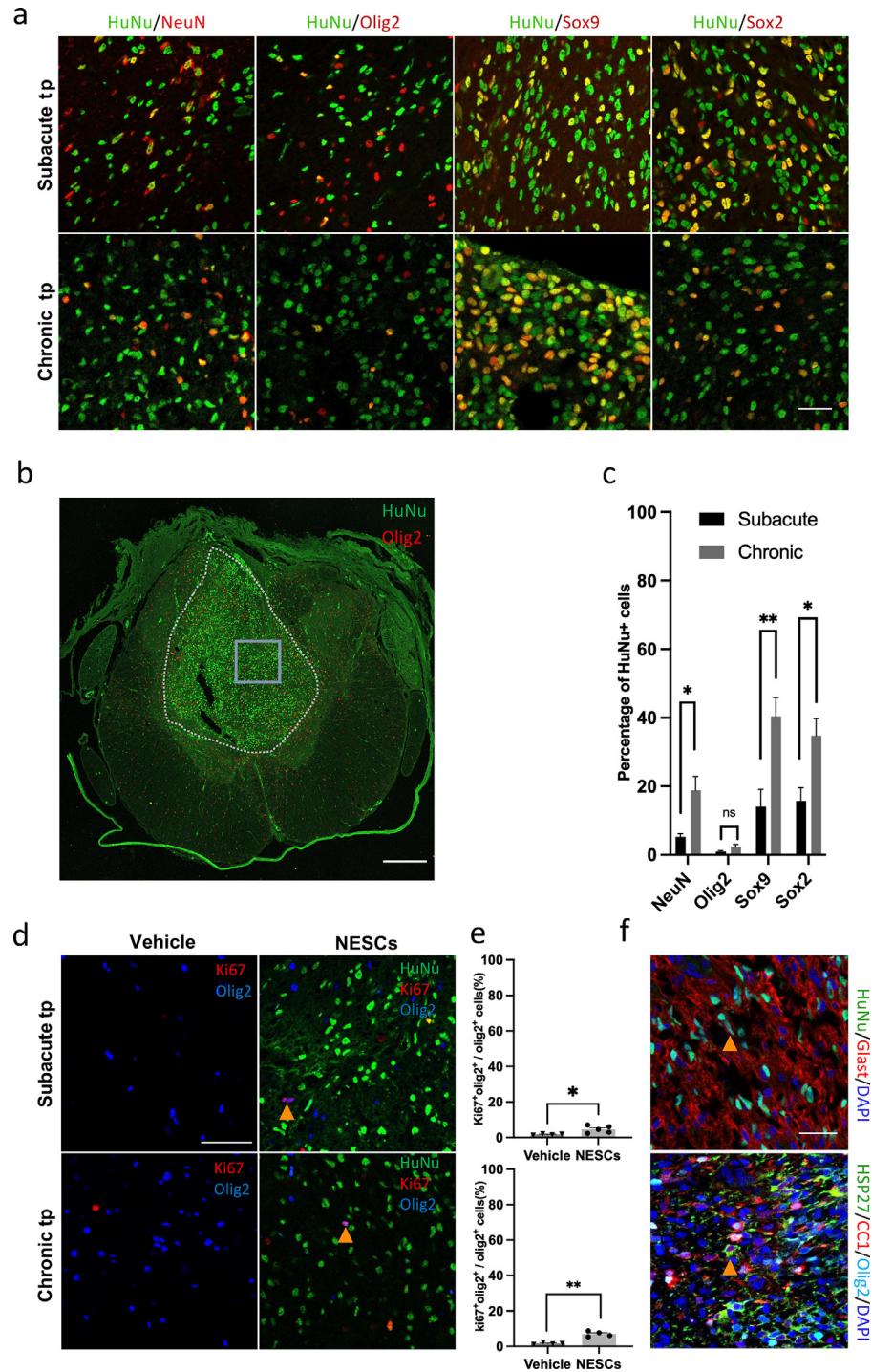


**Figure 4. NESC differentiated into multiple neural lineages after subacute and chronic transplantation.** (a) Spinal cord sections from the transplantation site stained for the indicated markers. Scale bar = 30  $\mu$ m. (b) Overview of the spinal cord with transplant, stained for the indicated markers. Scale bar = 300  $\mu$ m. (c) Quantification of the fates of NESC (mean  $\pm$  SEM, two-tailed t-test,  $p < 0.05$ , no statistical significance,  $p < 0.01$  and  $p < 0.05$  for the respective phenotype). (d) Spinal cord sections of transplantation sites of vehicle and NESC groups 10 weeks after subacute and chronic transplantation, stained for HuNu (green), Olig2 (blue) and Ki67 (red). Scale bar = 50  $\mu$ m. Arrowheads show proliferating OPCs. (e) Quantification of proliferating OPCs (Olig2<sup>+</sup>/Ki67<sup>+</sup>) as described in (d) (mean  $\pm$  SEM, two-tailed t-test,  $p < 0.05$ ,  $n = 4$  and 5 rats per group 10 weeks after subacute transplantation) and (mean  $\pm$  SEM, two-tailed t-test,  $p < 0.01$ ,  $n = 4$  rats per group 10 weeks after chronic transplantation). (f) Spinal cord sections of transplantation site stained for indicated markers. Scale bar = 30  $\mu$ m. Section thickness = 10  $\mu$ m.

subtype.<sup>23,24</sup> Therefore, we investigated whether NESCs could affect CSPG<sub>4</sub> distribution in the same way as they modified the astrocytic scars. We found that the wall of cyst was strongly CSPG<sub>4</sub> immunoreactive in rats from the vehicle group, while the CSPG<sub>4</sub> positive layers were absent in rats that received NESC transplantation (Figure 5 b).

We also analyzed if transplanted NESCs affected active microglia/macrophages, critical mediators of inflammation, which can contribute to tissue degeneration in chronic SCI. Both activated microglia and activated infiltrating macrophages from periphery monocytes are recognized by the transition from a ramified morphology to a rounded, amoeboid shape with expression of ED1. We quantified the number of ED1 positive cells and found that 10 weeks after subacute as well as chronic transplantation of NESCs, the number of ED1 positive cells was significantly lower compared to the vehicle groups (Figure 5 g). Moreover, most of the ED1 positive cells at lesion sites from both subacute and chronic transplantation groups (both NESCs and vehicle) were activated with round shape (Figure 5 f). To further define the local inflammation state, we investigated two pro-inflammatory cytokines interleukin-1 $\beta$  (IL-1 $\beta$ ) and tumor necrosis factor alpha (TNF $\alpha$ ) and one anti-inflammatory cytokine interleukin-1 receptor antagonist (IL1RA). We found both IL-1 $\beta$  and TNF $\alpha$  were colocalized with GFAP in astrocytes, as was reported previously by Ji et al.<sup>25</sup> Consequently, the alteration of IL-1 $\beta$  and TNF $\alpha$  was paralleled by the changes in GFAP in both subacute transplantation and chronic transplantation, with a reduction by NESCs only in subacute transplantation (Figure S6 and S7). On the other hand, IL1RA was mainly expressed in ED1 positive microglia/macrophages in both vehicle and NESCs groups in subacute and chronic transplantation. Although the average percentage of IL1RA was higher in the NESCs group than the vehicle group, this difference was not significant (Figure S8).

### Axonal regrowth was promoted by the transplantation of NESCs

With our findings that transplanted NESCs reduced the astroglial scar tissue, the presence of growth inhibitory molecule CSPG<sub>4</sub> surrounding the lesion site, and the number of active microglia/macrophages, we decided to investigate if this resulted in enhanced axonal regeneration by quantifying the density of descending serotonergic (5-HT) positive axons below the injury. In the NESCs group, we found that there were 5-HT positive axons growing into the transplant (Figure 6 a) and at least 4 mm caudal to the lesion site. The 5-HT positive axons only extended 1mm caudal to the lesion site in the vehicle group. When we quantified 5-HT positive axons 2 mm caudal to the lesion site, we found that the

density of 5-HT positive axons in rats transplanted with NESCs either subacutely into parenchyma or chronically into the PTS cysts was significantly higher than the corresponding vehicle group (Figure 6 b and c).

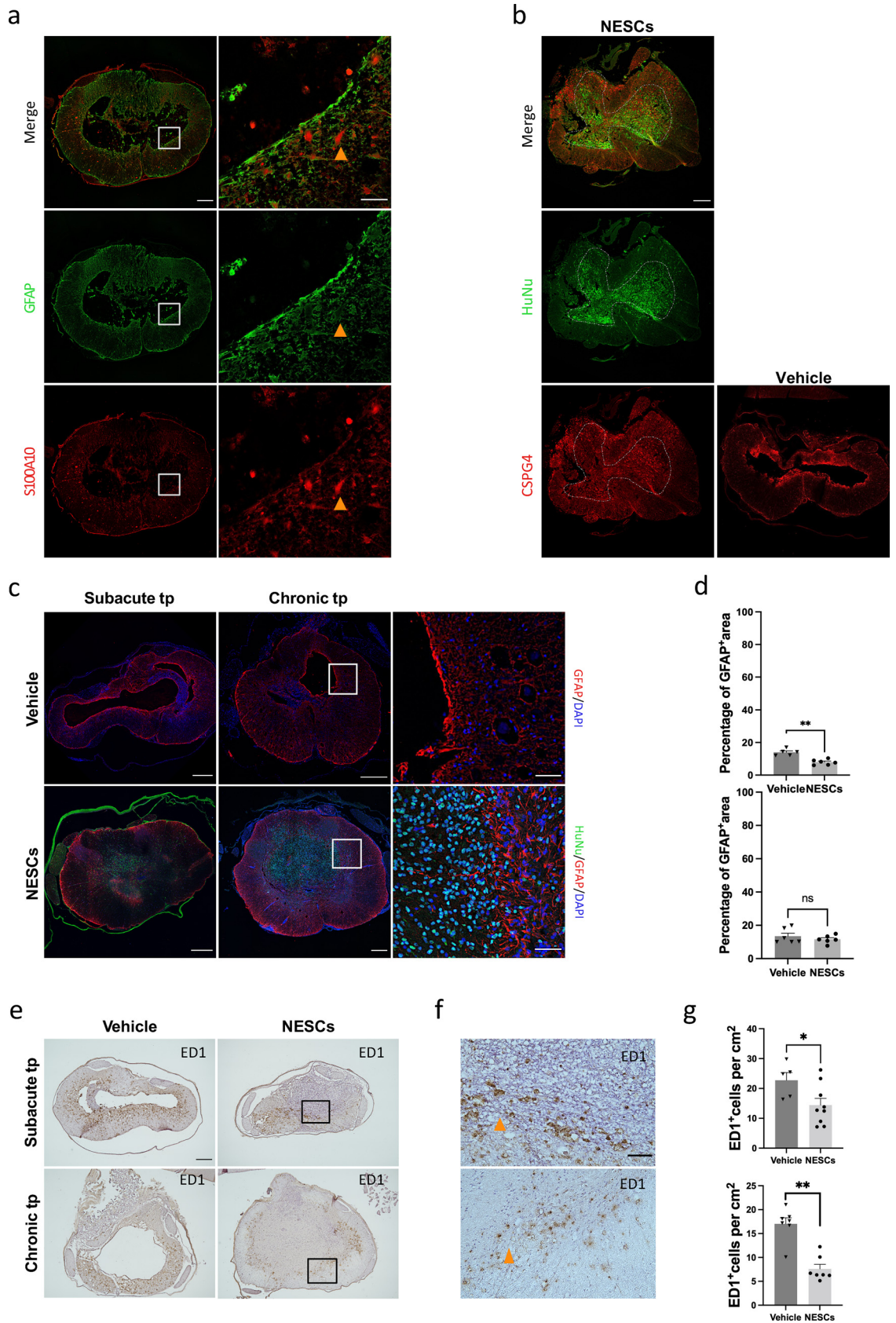
### Discussion

Clinically, the treatment for PTS patients with progressive symptoms is limited to surgical intervention to restore the normal flow of cerebrospinal fluid by detaching and to collapse the cyst by shunting. However, a recent systematic review concluded that “no satisfactory standard treatment exists”.<sup>26</sup> We hypothesize that transplantation of neural stem and progenitor cells in conjunction with surgical treatment results in higher efficacy. In our previous study, we demonstrated that human NPCs derived either from prenatal tissue or iPSCs (i.e., NESCs) effectively reversed intraspinal cyst expansion in a rat model of PTS,<sup>15</sup> but if these transplanted cells can also achieve tissue repair has not been studied.

In the present study, we used NESCs derived from GMP-compliant iPSCs, and optimized cell preparation for transplantation by using cryopreserved NESCs right after thawing. These NESCs showed similar high viability as non-frozen NESCs (data not shown), making them easier to use in a clinical setting. To analyze the fate of NESCs 10 weeks after transplantation, and what effects they have on the injured spinal cord both subacutely and chronically, we transplanted NESCs to PTS rats 1 or 10 weeks after injury, and found that (i) off-the-shelf cryo-preserved NESCs survived, proliferated, and differentiated into the major neural lineages in both transplantation conditions, (ii) the intraspinal cyst expansion was prevented by NESCs when transplanted chronically, and that the development of cysts was prevented by subacute transplantation, (iii) the host tissue responded to the NESC transplantation with an extensive proliferation of OPCs with the migration of OPCs into the graft and (iv) the glial scar was reduced, expression of the neurite inhibitory molecule CSPG<sub>4</sub> suppressed, which was associated with regeneration of descending serotonergic axons, the latter two effects achieved in both transplantation conditions.

The safety and survival of transplanted cells are basic requirements for clinical translation of cell therapy.<sup>27,28</sup> One of the major safety concerns of transplantation of stem/progenitor cells is tumorigenicity. A previous study showed the risk of teratoma formation applying iPSC-derived cells.<sup>29</sup> Since viral reprogramming is associated with tumorigenicity, we used non-inserting mRNAs to induce pluripotency.<sup>30</sup> We confirmed the safety of the NESCs derived from these iPSCs *in vivo* since we found no signs of tumor growth in transplanted rats. Most of the transplanted cells remained at the implantation site with limited migration to surrounding intact tissue, and no signs of ectopic colonies.







The average proliferation rate of transplanted NESCs decreased rapidly as expected over time, similar to what we observed previously for human fetal NPCs,<sup>11</sup> and we could not find clusters of cells with unexpectedly high proliferation rates. The other safety issue is the origin of reagents and the risk of microbiological contamination. To address this, we used culture reagents that were xeno-free.<sup>31</sup> NESCs have good survival after subacute as well as chronic transplantation. We found more human cells after chronic than subacute transplantation, which could simply be due to there being more space available for transplanted cells (due to the tissue loss).

Considering the loss of neural parenchyma after SCI, further aggravated by the cyst expansion, the potency of NESCs (and other NPCs) to differentiate into several neural lineages is necessary if some of this tissue is to be replaced, and lost neural circuitry recreated. The grafted NESCs were indeed capable of differentiating into the major neural cell lineages. However, in our study, the differentiation rate of NESCs was 30% and 60% in subacute and chronic transplantation, respectively, which are lower than other published studies. The ratio of the neuron to glial cells was also lower. In a study with a similar cell line, 70% of surviving NESCs differentiated into TuJ1 positive neurons and 18% into GFAP positive astrocytes at 4 weeks post-transplantation in a mouse SCI model and 60% to neurons and 10% to astrocytes in another study of iPSC-derived NPCs.<sup>32,33</sup> These studies differ with respect to animal models used, time of implantation and other factors that may be relevant. One possible factor influencing differentiation is inflammatory activity, which is more pronounced in the spinal cord of PTS rats compared to SCI.<sup>34</sup> Inflammation suppresses differentiation of NPCs, reduces neurogenesis, and enhances astrogliogenesis.<sup>35,36</sup> This effect may also contribute to the lower rate of differentiation after subacute transplantation compared to chronic, since inflammation is more severe in the subacute phase of SCI,<sup>37</sup> although other factors most likely also affect differentiation.

Despite the limited differentiation, NESCs effectively counteracted cyst pathology after subacute and chronic transplantation. It is possible that one of the main therapeutic mechanisms of NESCs is to reduce the density of active microglia/macrophages and reactive astrocytes, since they act in synergy to enhance the intensity of the

inflammation. Reduced inflammation could result in better tissue preservation and thereby probably suppress cyst formation in the subacute phase and cyst expansion in the chronic phase. As expected, the reduced GFAP positive astrocytes were accompanied by a reduction of IL-1 $\beta$  and TNF $\alpha$  in subacute NESC transplantation. The suppression of inflammation brought about by NESCs is probably an important mechanism of tissue preservation in subacute transplantation since inflammation is a major secondary injury in SCI.<sup>38,39</sup> Considering the lack of significant change in the anti-inflammatory cytokines IL1RA, it most likely plays a minor role, if any, in the treatment effects by NESCs. Another possible therapeutic mechanism is the reduction of aquaporin 4 in astrocyte cell membranes by acute and chronic NESC transplantation. Aquaporin 4 increase has been shown in a PTS model<sup>22</sup> suggesting it plays a role in cyst development. In addition, a more recent study showed that inhibition of aquaporin 4 translocation to the astrocyte cell surface largely prevented edema after SCI resulting in significant structural and functional improvement.<sup>40</sup> The cell graft will also fill parts of the cysts with human cells after chronic transplantation. This effect is, however, small since the total volume of the cell graft is at least one order of magnitude smaller than the volume reduction. Based on the present data and our previous study,<sup>15</sup> the reduction in cyst volume brought about by NESC transplantation is a combined effect of the addition of grafted NESCs and their progeny, proliferating host cells, and also a major reduction in the amount of cyst fluid, probably due to a change in flow dynamics within the spinal cord, partly caused by changes of aquaporin 4 expression.

In addition to the pronounced effect of NESC implantation on cyst size, we found that these cells have major effects on neural tissue repair. NESCs increase the proliferation of endogenous OPCs, stimulate migration and differentiation to oligodendrocytes, possibly evoked by growth factors released from the NESCs.<sup>41</sup> The newly formed oligodendrocytes may remyelinate the injured axons and restore their conductivity. Generation of myelin-forming oligodendrocytes have been enhanced in mouse models of SCI using genetic methods,<sup>42</sup> but these strategies are still very challenging for clinical translation. In addition, the non-differentiated OPCs have functions beyond remyelination, such as

**Figure 5. Reactive astrocytes and scar-forming astrocytes were affected by transplanted NESCs.** (a) Spinal cord sections of lesion sites from vehicle treated rats in chronic transplantation condition showing a large cyst surrounded by parenchyma stained for GFAP (green) and S100A10 (red). (b) Spinal cord sections of lesion site from vehicle and NESCs groups after chronic transplantation stained for HuNu (green), CSPG4 (red) and DAPI (blue). (c) Spinal cord sections of lesion sites stained for HuNu (green) and GFAP (red) from both vehicle and NESCs groups 10 weeks after subacute or chronic transplantation. (d) Quantification of the GFAP positive area to whole section of the experiment illustrated in b (mean  $\pm$  SEM, two-tailed t-test, subacute:  $p < 0.01$ ,  $n = 5$  and 6 rats, respectively, chronic: no statistical significance,  $n = 6$ ). (e) Spinal cord sections of lesion sites from vehicle and NESCs groups 10 weeks after subacute or chronic transplantation stained for ED1. (f) Magnified image of the boxed area in e. (g) Quantification of ED1 positive cells 10 weeks after subacute or chronic transplantation as described in E (mean  $\pm$  SEM, two-tailed t-test, subacute:  $p < 0.05$ ,  $n = 5$  and 9 rats, respectively, chronic:  $p < 0.05$ ,  $n = 7$  rats per group). Section thickness = 10  $\mu$ m.

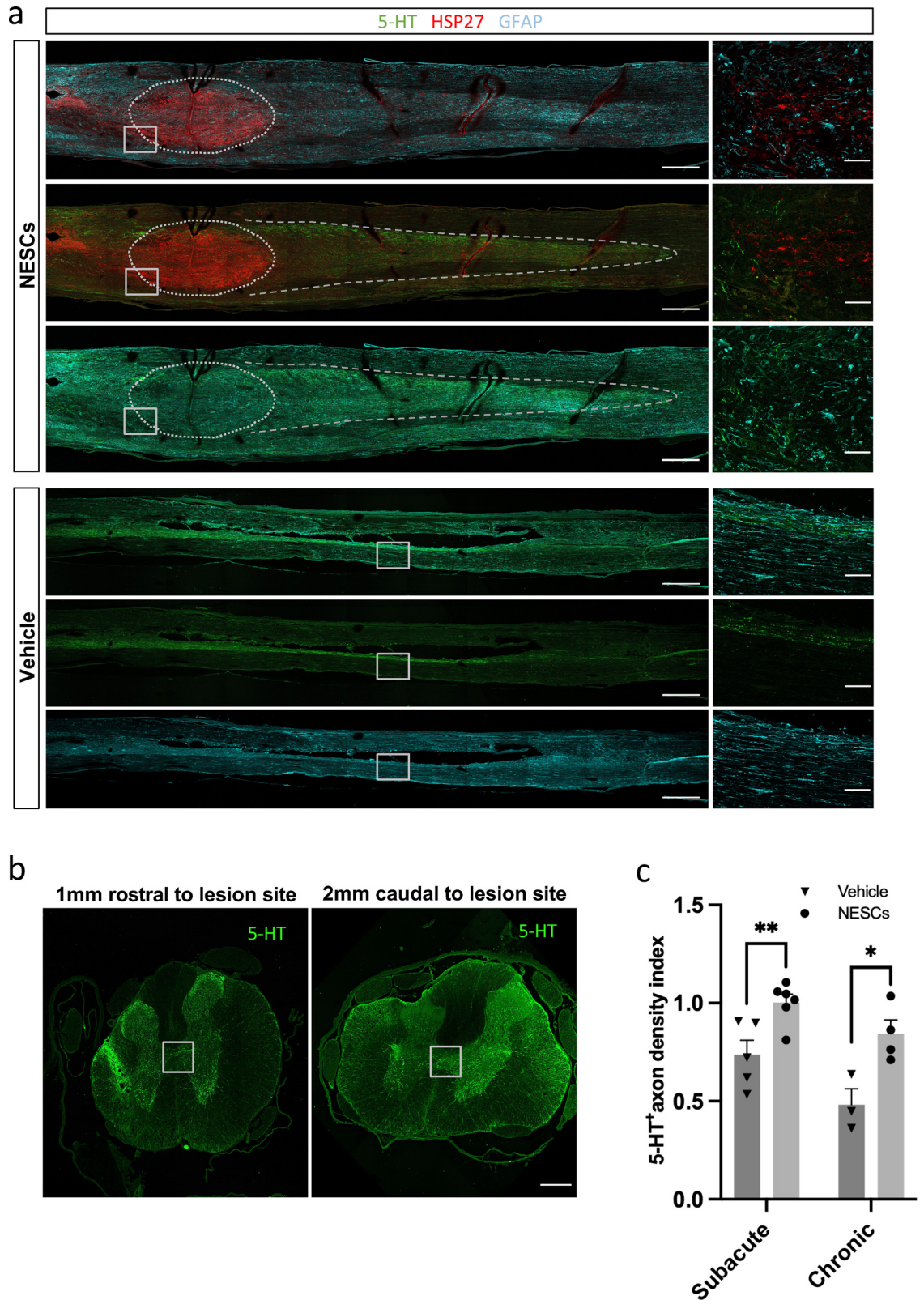


**Figure 6.** NESCs promote axon regrowth in both subacute and chronic transplantation conditions. (a) Longitudinal sections of spinal cord along the midline from both vehicle and NESCs groups 10 weeks after chronic transplantation and stained for 5-HT

maintenance of homeostatic microglia which partly contribute to tissue repair.<sup>43</sup> Therefore, the capacity of NESCs to stimulate proliferation and migration of OPCs are features that most likely can contribute to repair of the injured spinal cord.

Functional axonal regrowth hardly occurs in SCI due to intrinsic and extrinsic factors, and a large number of studies have addressed how to control factors suggested to prevent regrowth.<sup>20,44</sup> In our study, we observed that NESCs transplantation led to a significant reduction of the astrocytic scars and CSPG4 positive immunoreactivity surrounding the lesion core after subacute and chronic NESCs transplantation. Similar effects on astrocytic scars have been observed in other transplantation studies of neural stem cells.<sup>45</sup> It is most likely that the attenuated glial scar and reduced presence of CSPG4 are the main reasons for the regrowth of serotonergic axons that we observed. Serotonergic axons are important for modulating motor, sensory and autonomic function in rodents, and their regrowth by NPC treatment in SCI has previously been demonstrated.<sup>46</sup> Our findings show that the serotonergic innervation of the spinal cord below the injury and cysts increases as a result of the NESC implantation, and that some regrowth occurs through the NESC graft in the PTS cyst. Although we cannot in the present study determine if regrowth occurs from severed axons (regeneration) or spared axons (sprouting), reinnervation of the caudal spinal cord clearly occurs.

In summary, by transplanting NESCs derived from GMP-compliant iPSCs and using them as off-the-shelf therapy to a clinically relevant rat model of PTS, we found pronounced treatment effects that can prevent cyst expansion in the chronic transplantation, and prevention of cyst formation after subacute transplantation. In addition, we identified several therapeutic effects associated with tissue repair, including promoting host OPC proliferation and differentiation, suppressing inflammation, reducing glial scar and expression of neurite inhibitory CSPG4 and enhancing regrowth of descending serotonergic axons. These effects could enhance long-term recovery in PTS patients, beyond the urgent elimination of the intramedullary cysts. While the differentiation of transplanted NESCs was limited, the differentiated progeny may add to the repair of the injured spinal cord. More extensive differentiation of the grafted NESCs may provide more pronounced tissue replacement. But in attempts to increase *in vivo* differentiation of NESCs in PTS for example using

pre-differentiation or treatment with notch inhibitors with the aim to replace lost neurons,<sup>18,47</sup> it is critical to make sure that the tissue repair effects we now identified are not lost.

### Contributors

Conception and design of study-Tingting Xu, Xiaofei Li, Anna Falk, and Erik Sundström; Acquisition, analysis, and verification of data-Tingting Xu, Yuxi Guo, Elias Uhlin, Lena Holmberg, Dania Winn, and Sumonto Mitra; Writing&Editing-Tingting Xu, Xiaofei Li, Yuxi Guo, Erik Sundström, Anna Falk, Dania Winn. All authors read and approved the final version of the manuscript.

### Data sharing statement

Data are available upon reasonable request by sending a message to the corresponding author.

### Declaration of interests

The authors declare no competing interests.

### Acknowledgments

This study was supported financially by Vinnova (2016-04134), Karolinska Institutet StratRegen, and Chinese Scholarship Council (CSC). We acknowledge the expert technical assistance with micro-MRI by staff from the Karolinska Experimental Research and Imaging Center (KERIC). We acknowledge Dr. Stefan Svensson for sharing the homemade IL1RA antibodies.

### Supplementary materials

Supplementary material associated with this article can be found in the online version at doi:[10.1016/j.ebiom.2022.103882](https://doi.org/10.1016/j.ebiom.2022.103882).

### References

- 1 Kim HG, Oh HS, Kim TW, Park KH. Clinical features of post-traumatic syringomyelia. *Korean J Neurotrauma*. 2014;10(2):66–69.
- 2 Squier MV, Lehr RP. Post-traumatic syringomyelia. *J Neurol Neurosurg Psychiatry*. 1994;57(9):1095–1098.
- 3 Scivoletto G, Masciullo M, Pichiorri F, Molinari M. Silent post-traumatic syringomyelia and syringobulbia. *Spinal Cord Ser Cases*. 2020;6(1):15.

(green), HSP27 (red) and GFAP (cyan). Scale bar= 400  $\mu$ m. (b) Representative coronal sections of the spinal cord 1 mm rostral and 2 mm caudal to a lesion site 10 weeks after subacute transplantation of NESCs, stained for 5-HT (green). Scale bar= 50  $\mu$ m. (c) Quantification of 5-HT positive axons in both vehicle and NESCs groups 10 weeks after subacute or chronic transplantation (mean  $\pm$  SEM, two-tailed t-test,  $p < 0.01$ ,  $n = 5$  and 6 rats, respectively) and 10 weeks after chronic transplantation (mean+ SEM, two-tailed t-test,  $p < 0.05$ ,  $n = 3$  and 4 rats, respectively). 5-HT positive axon density index is the ratio of 5-HT density from 2 mm caudal to the injury site to 1mm rostral to the injury site. Section thickness = 10  $\mu$ m.



- 4 Qiu Y, Zhu ZZ, Lu JY, Wang B, Li WG, Zhu LH. Clinical manifestations and significance of post-traumatic thoracolumbar syringomyelia. *Chin J Traumatol*. 2004;7(1):52–55.
- 5 Schaan M, Jaksche H. Comparison of different operative modalities in post-traumatic syringomyelia: preliminary report. *Eur Spine J*. 2001;10(2):135–140.
- 6 Leahy HP, Beckley AA, Formal CS, Fried GW. Post-traumatic syringomyelia refractory to surgical intervention: a series of cases on recurrent syringomyelia. *Spinal Cord Ser Cases*. 2015;1:15013.
- 7 Curtis E, Martin JR, Gabel B, et al. A first-in-human, phase I study of neural stem cell transplantation for chronic spinal cord injury. *Cell Stem Cell*. 2018;22(6):941–950. e6.
- 8 Ceto S, Sekiguchi KJ, Takashima Y, Nimmerjahn A, Tuszyński MH. Neural stem cell grafts form extensive synaptic networks that integrate with host circuits after spinal cord injury. *Cell Stem Cell*. 2020;27(3):430–440. e5.
- 9 Lige L, Zengmin T. Transplantation of neural precursor cells in the treatment of Parkinson disease: an efficacy and safety analysis. *Turk Neurosurg*. 2016;26(3):378–383.
- 10 Salewski RP, Mitchell RA, Shen C, Fehlings MG. Transplantation of neural stem cells clonally derived from embryonic stem cells promotes recovery after murine spinal cord injury. *Stem Cells Dev*. 2015;24(1):36–50.
- 11 Emgard M, Piao J, Aineskog H, et al. Neuroprotective effects of human spinal cord-derived neural precursor cells after transplantation to the injured spinal cord. *Exp Neurol*. 2014;253:138–145.
- 12 Sareen D, Gowing G, Sahabian A, et al. Human induced pluripotent stem cells are a novel source of neural progenitor cells (iNPCs) that migrate and integrate in the rodent spinal cord. *J Comp Neurol*. 2014;522(12):2707–2728.
- 13 Ishii T, Eto K. Fetal stem cell transplantation: past, present, and future. *World J Stem Cells*. 2014;6(4):404–420.
- 14 Wei D, Yamoah EN. Regeneration of the mammalian inner ear sensory epithelium. *Curr Opin Otolaryngol Head Neck Surg*. 2009;17(5):373–380.
- 15 Xu N, Xu T, Mirasol R, et al. Transplantation of human neural precursor cells reverses syrinx growth in a rat model of post-traumatic syringomyelia. *Neurotherapeutics*. 2021.
- 16 Kadoya K, Lu P, Nguyen K, et al. Spinal cord reconstitution with homologous neural grafts enables robust corticospinal regeneration. *Nat Med*. 2016;22(5):479–487.
- 17 Kumamaru H, Kadoya K, Adler AF, et al. Generation and post-injury integration of human spinal cord neural stem cells. *Nat Methods*. 2018;15(9):723–731.
- 18 Okubo T, Nagoshi N, Kohyama J, et al. Treatment with a gamma-secretase inhibitor promotes functional recovery in human iPSC-derived transplants for chronic spinal cord injury. *Stem Cell Rep*. 2018;11(6):1416–1432.
- 19 Suzuki H, Ahuja CS, Salewski RP, et al. Neural stem cell mediated recovery is enhanced by Chondroitinase ABC pretreatment in chronic cervical spinal cord injury. *PLoS One*. 2017;12(8):e0182339.
- 20 Hara M, Kobayakawa K, Ohkawa Y, et al. Interaction of reactive astrocytes with type I collagen induces astrocytic scar formation through the integrin-N-cadherin pathway after spinal cord injury. *Nat Med*. 2017;23(7):818–828.
- 21 Sun L, Li M, Ma X, et al. Inhibition of HMGB1 reduces rat spinal cord astrocytic swelling and AQP4 expression after oxygen-glucose deprivation and reoxygenation via TLR4 and NF-kappaB signaling in an IL-6-dependent manner. *J Neuroinflammation*. 2017;14(1):231.
- 22 Hemley SJ, Bilston LE, Cheng S, Chan JN, Stoodley MA. Aquaporin-4 expression in post-traumatic syringomyelia. *J Neurotrauma*. 2013;30(16):1457–1467.
- 23 Hussein RK, Mencio CP, Katagiri Y, Brake AM, Geller HM. Role of chondroitin sulfation following spinal cord injury. *Front Cell Neurosci*. 2020;14:208.
- 24 Kadesh IM, Arkhipova SS, Mukhamedshina YO, James V, Rizvanov AA, Chelyshev YA. The function of NG2/CSPG4-expressing cells in the rat spinal cord injury: an immunoelectron microscopy study. *Neuroscience*. 2021;467:142–149.
- 25 Ji XT, Qian NS, Zhang T, et al. Spinal astrocytic activation contributes to mechanical allodynia in a rat chemotherapy-induced neuropathic pain model. *PLoS One*. 2013;8(4):e60733.
- 26 Kleindienst A, Laut FM, Roewecklein V, Buchfelder M, Dodoo-Schittko F. Treatment of posttraumatic syringomyelia: evidence from a systematic review. *Acta Neurochir (Wien)*. 2020;162(10):2541–2556.
- 27 Stoddard-Bennett T, Pera RR. Stem cell therapy for Parkinson's disease: safety and modeling. *Neural Regen Res*. 2020;15(1):36–40.
- 28 Jafarzadeh Bejargafshe M, Hedayati M, Zahabiasli S, Tahmasbpour E, Rahmanzadeh S, Nejad-Moghaddam A. Safety and efficacy of stem cell therapy for treatment of neural damage in patients with multiple sclerosis. *Stem Cell Investig*. 2019;6:44.
- 29 Tsuji O, Miura K, Fujiyoshi K, Momoshima S, Nakamura M, Okano H. Cell therapy for spinal cord injury by neural stem/progenitor cells derived from iPS/ES cells. *Neurotherapeutics*. 2011;8(4):668–676.
- 30 Mohamad O, Drury-Stewart D, Song M, et al. Vector-free and transgene-free human iPS cells differentiate into functional neurons and enhance functional recovery after ischemic stroke in mice. *PLoS One*. 2013;8(5):e64160.
- 31 Vitillo L, Durance C, Hewitt Z, Moore H, Smith A, Vallier L. GMP-grade neural progenitor derivation and differentiation from clinical-grade human embryonic stem cells. *Stem Cell Res Ther*. 2020;11(1):406.
- 32 Fujimoto Y, Abematsu M, Falk A, et al. Treatment of a mouse model of spinal cord injury by transplantation of human induced pluripotent stem cell-derived long-term self-renewing neuroepithelial-like stem cells. *Stem Cells*. 2012;30(6):1163–1173.
- 33 Kajikawa K, Imaizumi K, Shinozaki M, et al. Cell therapy for spinal cord injury by using human iPSC-derived region-specific neural progenitor cells. *Mol Brain*. 2020;13(1).
- 34 Austin JW, Afshar M, Fehlings MG. The relationship between localized subarachnoid inflammation and parenchymal pathophysiology after spinal cord injury. *J Neurotrauma*. 2012;29(10):1838–1849.
- 35 Borsini A, Zunszain PA, Thuret S, Pariante CM. The role of inflammatory cytokines as key modulators of neurogenesis. *Trends Neurosci*. 2015;38(3):145–157.
- 36 Wu MD, Montgomery SL, Rivera-Escalera F, Olschowka JA, O'Banion MK. Sustained IL-1beta expression impairs adult hippocampal neurogenesis independent of IL-1 signaling in nestin+ neural precursor cells. *Brain Behav Immun*. 2013;32:9–18.
- 37 Trivedi A, Olivas AD, Noble-Haeusslein LJ. Inflammation and spinal cord injury: infiltrating leukocytes as determinants of injury and repair processes. *Clin Neurosci Res*. 2006;6(5):283–292.
- 38 Boato F, Rosenberger K, Nelissen S, et al. Absence of IL-1beta positively affects neurological outcome, lesion development and axonal plasticity after spinal cord injury. *J Neuroinflammation*. 2013;10:6.
- 39 Ijaz S, Mohammed I, Gholaminejad M, Mokhtari T, Akbari M, Hassanzadeh G. Modulating pro-inflammatory cytokines, tissue damage magnitude, and motor deficit in spinal cord injury with subventricular zone-derived extracellular vesicles. *J Mol Neurosci*. 2020;70(3):458–466.
- 40 Kitchen P, Salman MM, Halsey AM, et al. Targeting aquaporin-4 subcellular localization to treat central nervous system edema. *Cell*. 2020;181(4):784–799. e19.
- 41 Bribian A, Medina-Rodriguez EM, Josa-Prado F, et al. Functional heterogeneity of mouse and human brain OPCs: relevance for pre-clinical studies in multiple sclerosis. *J Clin Med*. 2020;9(6).
- 42 Llorens-Bobadilla E, Chell JM, Le Merre P, et al. A latent lineage potential in resident neural stem cells enables spinal cord repair. *Science*. 2020;370(6512).
- 43 Zhang SZ, Wang QQ, Yang QQ, et al. NG2 glia regulate brain innate immunity via TGF-β2/TGFBR2 axis. *BMC Med*. 2019;17(1):204.
- 44 Anderson MA, O'Shea TM, Burda JE, et al. Required growth facilitators propel axon regeneration across complete spinal cord injury. *Nature*. 2018;561(7723):396–400.
- 45 Lien BV, Tuszyński MH, Lu P. Astrocytes migrate from human neural stem cell grafts and functionally integrate into the injured rat spinal cord. *Exp Neurol*. 2019;314:46–57.
- 46 Perrin FE, Noristani HN. Serotonergic mechanisms in spinal cord injury. *Exp Neurol*. 2019;318:174–191.
- 47 Abeyinghe HC, Bokhari L, Quigley A, et al. Pre-differentiation of human neural stem cells into GABAergic neurons prior to transplant results in greater repopulation of the damaged brain and accelerates functional recovery after transient ischemic stroke. *Stem Cell Res Ther*. 2015;6:186.